Mechanical and physical properties of selected magnesium base nanocomposites

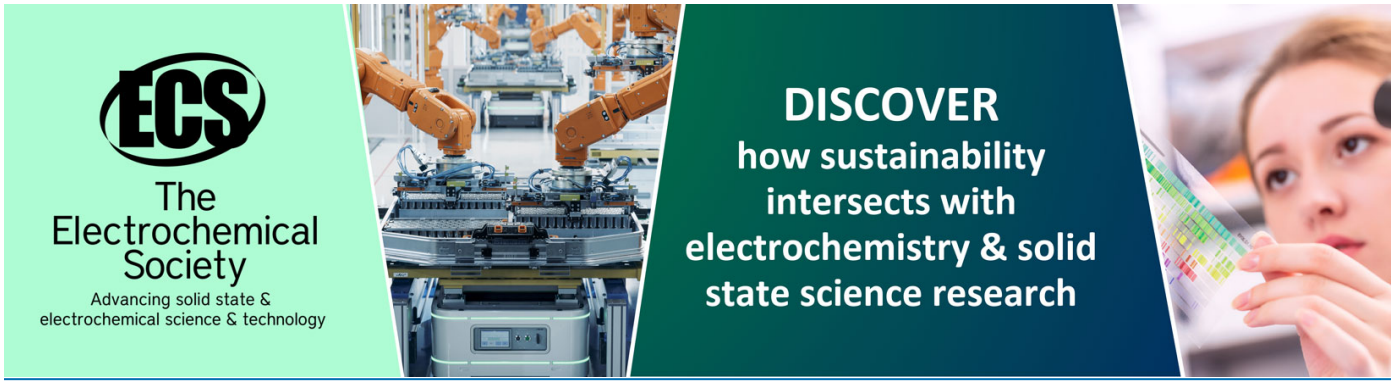

IOP Conf. Series: Materials Science and Engineering **372** (2018) 012004 doi:10.1088/1757-899X/372/1/012004

Mechanical and physical properties of selected magnesium base nanocomposites

Z Drozd[1,3], Z Trojanová[1], P Lukáč[1], M Kučeráková[2] and T Václavů[2]

[1]Faculty of Mathematics and Physics, Charles University, Ke Karlovu 3, CZ-121 16 Prague 2, Czech Republic
[2]Department of Structure Analysis, Institute of Physics of the Czech Academy of Sciences, Cukrovarnická 10, CZ-162 00 Prague 6, Czech Republic

E-mail: zdenek.drozd@mff.cuni.cz

Abstract. The effect of various nanoparticles (BN, Al_2O_3, ZrO_2, Gr) on the mechanical and physical properties of magnesium was studied in the present paper. Microcrystalline magnesium reinforced with nanoparticles was prepared by ball milling and hot extrusion. Microhardness of samples was measured at room temperature. The linear thermal expansion of the nanocomposites was measured over a wide temperature range from RT up to 400°C. Dynamic modulus and amplitude dependent internal friction were measured at room temperature. Although all nanocomposites were prepared with the same technology substantial differences in mechanical and physical properties were estimated among various nanocomposites. Bonding between magnesium matrix and ceramic and graphite nanoparticles plays important role for the resulting nanocomposites properties.

1. Introduction

Magnesium alloys and composites are very attractive materials due to their good properties: low density, high specific stiffness and good creep resistance. These properties nominate Mg materials predominantly for applications where low weight is required. On the other hand, there is a big competition of aluminum alloys in this field. One possibility of further improvement of Mg is adding of ceramic particles or fibres. By this process composite microstructure – metal matrix composite (MMC) can be obtained. MMCs provide promising solution for various structural applications. Such composites have much better mechanical properties in comparison with unreinforced materials. The special types of MMCs are so called nanocomposites. Nanocomposites (nc) combine two or more components where at least one of them has typical dimension in the nanometer region. Nanocomposites with the magnesium matrix exhibit improved strength, better creep resistance and they still have low density and good machinability [1,2].

It is known that addition of the second phase (e.g. SiC, MgO, Al_2O_3) with a micrometer size improves properties of the matrix itself (yield strength, elastic moduli, hardness, damping, thermal properties and so on) [1-6]. Using of nano-reinforcements can bring many interesting improvements as it has been reported in [7-9].

Magnesium composites with the micrometer-size reinforcements have usually lower ductility caused by the crack of the reinforcements which occurs at the particle-matrix interface and also by the voids in the vicinity of the interfaces. Presence of the voids at the interface play role also in the process of crack initiation. The improvement of the composites properties can be caused by the hot extrusion

manufacturing process. Certain consolidation of the composite and homogenization of the reinforcing phase is usually achieved using this technology. On the other hand, hot extrusion can increase the probability of particle fracture.

Recently reported experimental results indicated, that in the case of nanometer-scaled reinforcing phase some improvement of the mechanical properties occurred without a loss of ductility [10-13]. It has been also reported that a small volume fraction of nanoparticles (np) resulted in the comparable or better properties comparing the case of composites with the higher volume fraction of micro scaled reinforcements. Quite effective reinforcing effect of nanoparticles was found in the nanocomposites with Al_2O_3 particulates; as it was reported by Hassan et al [14]. Authors estimated that the nano-reinforcements improve the dimensional stability of pure Mg. The thermally stable alumina (Al_2O_3) nanoparticles (np) cause a significant increase in the microhardness at room temperature, enhance of dynamic elastic modulus as well as the yield strength, ultimate tensile strength and ductility of the material. This effect was observed up to 150 °C. There are several possible mechanisms describing the effect of nanoparticles on the plastic deformation of the nanocomposites [15]. Following process can be taken into account: an increase of the grain boundary area caused by a certain grain refinement, an increase of the dislocation density which accommodates the thermal stresses generated at the particle/matrix interface – such stresses occur due to the difference in the thermal expansion coefficients between the reinforcement phase and the matrix metal and good transfer of the applied stress in the case of effective particle-matrix binding. The Orowan strengthening as well as generation of geometrically necessary dislocations which accommodate the reinforcement/matrix interface during the plastic deformation should also play not negligible role. The distribution of particles in nanocomposites is usually not uniform. The clusters of nanoparticles are often formed. Clusters of various sizes can be found at the vicinity of grain boundaries. This fact represents a serious problem for modeling of processes in the nanocomposites. Despite great effort, no satisfying theoretical model describing the mechanical and physical properties of nanocomposites was developed. This is caused by the very complex character of this matter. Too many of factors and mechanisms play role and no satisfying complex research of these mechanisms has been done yet.

The properties of nanocomposites are influenced by the size, volume fraction and distribution of np and manufacturing technology. In this study, we reinforced pure magnesium with 3 vol.% of various np. All samples were prepared with the same technology. Mechanical and selected physical properties were estimated and compared in individual nanocomposites. Different strengthening effects of various np indicate that there is/are some other effect(s) influencing resulting properties of nanocomposites. We tried to find these hidden parameters which are important for the nc behavior.

2. Experimental

2.1. Materials preparation

Nanocomposites presented in this study - pure magnesium with 3 vol.% of various ceramic and graphite nanoparticles (Al_2O_3, ZrO_2, Gr and hexagonal BN-hBN) were prepared by the powder metallurgical route. In the first step magnesium powder was mixed and milled for 6 hr together with nanoparticles in a planetary ball mill with a speed of 150-200 rpm. Milled powder was then compacted under a pressure of 65 MPa. Hot extrusion (1:5.8 extruded ratio) of pre-compacted materials was next step of the preparation process. Rods of 12 mm in diameter were prepared using a horizontal 600 t extrusion press. Extrusion temperature was 350 °C; the extrusion speed exhibited value of 1.5 mm/s. In this paper the materials studied will be depicted as Mg+Al_2O_3 (Mg+ 3vol% alumina np) Mg+ZrO_2 (Mg+3vol% zirconia np), Mg+Gr (Mg+3vol.% graphite np) and Mg+BN (Mg+3vol.% hBN np).

TEM showed that the distribution of the nanoparticles was not homogenous. Particles were situated mainly in grain boundaries, only few particles were found within the grains.

2.2. Experimental methods

Microhardness was measured with the Vickers pyramid at room temperature in a Qness 10a apparatus

with the load of 0.1 kg. The dwell time was 10 s. Microhardness was estimated at the polished surface perpendicular to the extrusion direction. The indents were automatically evaluated along concentric circles as it is shown in figure 1. For the samples preparation the conventional mechanical polishing and etching were done using Glycol solution (1 ml HNO_3, 24 ml water, 75 ml ethylene glycol).

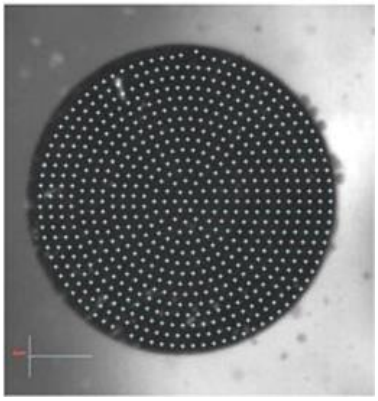

Figure 1. Microhardness measurements map.

Texture of samples was studied using scanning electron microscope ZEISS Auriga Compact equipped with EDAX EBSD camera; OIM software was utilized for EBSD observations. Samples were first mechanically grinded then polished with a diamond suspension of the grade 3.1 and ¼ μm and alumina suspension of the grade 0.05 μm. Finally, the samples surface was ion-polished by Leica EM RES102 device in order to get a high quality surface for EBSD measurements.

Characteristic stresses – offset compressive yield stress (CYS) and ultimate compression strength (UCS) were estimated from the true stress-true strain curves performed at room temperatures.

The thermal expansion was measured in an argon protective atmosphere using Netzsch 410 dilatometer in the temperature interval from room temperature up to 400 °C. The elongation of cylindrical samples with a diameter of 6 mm and 50 mm length were measured in an argon protective atmosphere. Four thermal cycles (heating-cooling) were performed with every specimen; the heating/cooling rate exhibited 0.9 K/min. The thermal expansion coefficient (CTE), α, was estimated as a derivative $\alpha=(1/\ell)\cdot(\mathrm{d}\ell/\mathrm{d}T)$, where, ℓ, is the sample length.

Young's modulus (YM) was estimated in a Resonant Frequency and Damping Analyser (RFDA). The cantilever beams were used for the modulus measurements. Samples were excited into resonant frequency using a small striker. Free vibrations of the sample were registered by a microphone. Fast Fourier transform was used to estimate the resonant frequency which served for the Young's modulus calculations. Amplitude dependent internal friction was measured at room temperature as damping of the sample free vibrations in a bending mode. Electromagnetic excitation and recording of vibrations was used. The resonant frequency exhibited ~ 40 Hz. The logarithmic decrement, δ, was used as a measure of the internal friction.

3. Results and discussion

Transmission electron micrograph of the Mg+Gr is reported in figure 2. The Gr nanoparticles form agglomerates which are situated mainly in the grain boundaries. Resulting materials after the hot extrusion exhibited very small grain size - units of micrometers. Grains were slightly elongated into the extrusion direction. Texture of Mg+BN and Mg+ZrO_2 nanocomposites is shown in figures 3(a) and 3(b), respectively. A typical ring texture was observed with the (0001) basal planes of the hexagonal cell parallel and <c> axis perpendicular to the extrusion direction. Such texture is typical for the hexagonal magnesium materials submitted to the hot extrusion.

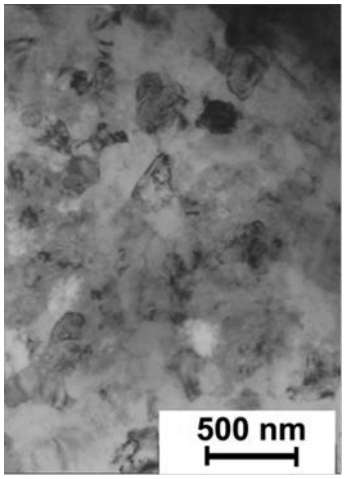

Figure 2. TEM micrograph of Mg+Gr nanocomposite.

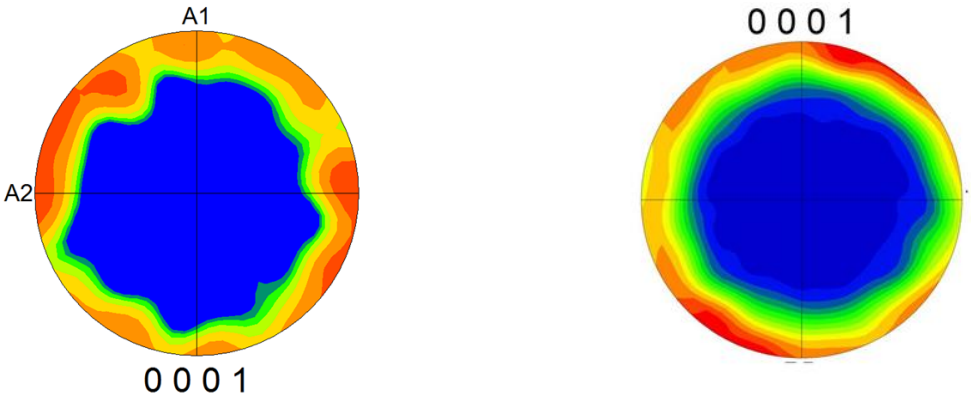

(a) (b)

Figure 3. (a) Pole figure of Mg+ZrO_2 nanocomposite and (b) Pole figure of Mg+BN nanocomposite.

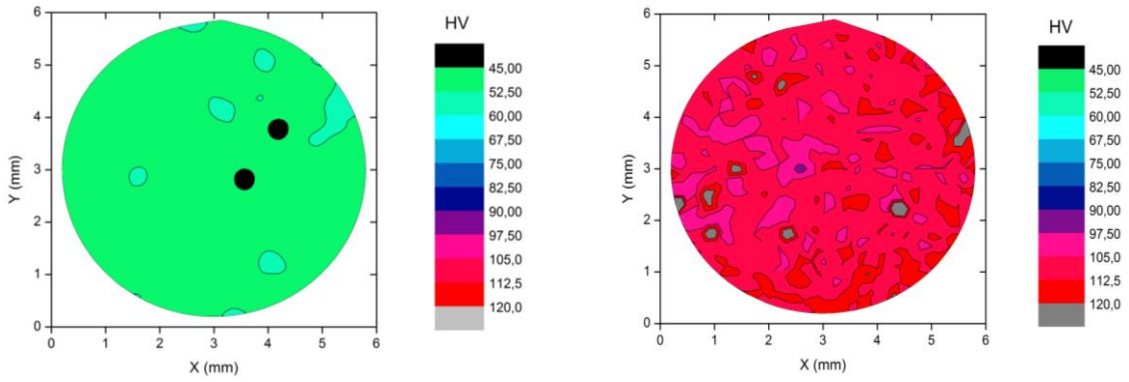

(a) (b)

Figure 4. Microhardness estimated for Mg+ZrO_2 (a), Mg+BN (b).

Vickers microhardness (HV) measured at room temperature in the samples cross-section is shown in figures 4(a) and 4(b) for Mg+ZrO_2 (a) and Mg+BN (b). Various colours of pictures indicate that microhardness of samples substantially differs. The mean HV values were: HV(Mg+ZrO_2) = 51.09±4.66 and HV(Mg+BN) = 110.2±4.66 i.e. practically two times higher compared with Mg+ZrO_2 sample.

Comparing HV values estimated for all nanocomposites, it can be seen that there is a big difference between both materials although they were prepared with the same method and contain 3 vol.% of ceramic nanoparticles.

Offset compressive yield stress (CYS) and ultimate compression strength (UCS) estimated at room temperature are given in table 1. Mechanical characteristics substantially vary for the materials studied.

Table 1. Compressive mechanical properties of Mg reinforced with different nanoparticles.

	Mg+Al_2O_3	**Mg+ZrO_2**	**Mg+Gr**	**Mg+BN**
CYS (MPa)	189	162	259	399
UCS (MPa)	413	236	293	406

Hardness, microhardness and mechanical properties of magnesium nanocomposites reinforced with alumina, zirconia and yttria nanoparticles were reported by several authors [1,6,13]. Comparing of experimental results is rather problematic because various preparation techniques and various contents of nanoparticles were used.

The temperature dependences of thermal expansion coefficient (CTE) estimated for microcrystalline Mg (μMg) and Mg+BN are shown in figure 5. The CTE values extrapolated to 20 °C are reported in table 2. It can be seen that the ceramic np decreased the thermal expansion. The values of CTE of the Mg+BN sample obtained from experiment were compared with the analytical prediction of the composite sample, α_C, by the rule of mixtures (RoM).

The rule of mixture may be written as

$$\alpha_c = (1 - V_p)\alpha_m + V_p\alpha_p \quad (1)$$

where α_c, α_m and α_p are the CTEs of the composite, matrix, and particle, respectively, and V_p is the volume fraction of the reinforcing phase particles. Comparing calculated CTE-value according to rule of mixtures good agreement with the experimentally estimated value can be seen (table 2).

Table 2. Thermal expansion coefficient (CTE) and Young`s modulus (E) estimated at room temperature.

	μMg	**Mg+BN**	**pkMg**	**hBN**
CTEx$10^{-6}K^{-1}$	24.38	23.55	25.38	4.56
CTE(RoM)x$10^{-6}K^{-1}$		23.79		
E(GPa)	44.15	48.80	43.1	675

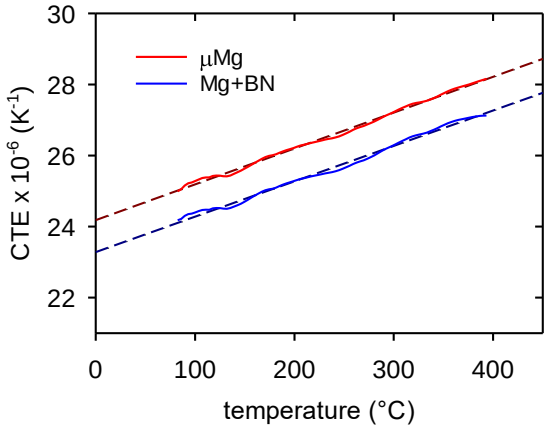

Figure 5. Temperature dependence of CTE.

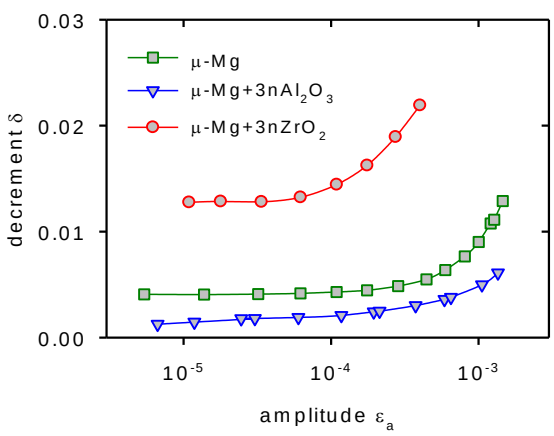

Figure 6. Strain amplitude dependence of decrement.

Experimental values of Young`s moduli for polycrystalline magnesium (pkMg) and hBN were taken from literature [16-18]. Good agreement between measured values of CTE and calculated according rule of mixture is very probably a consequence of the good bonding between matrix and the reinforcing phase nanoparticles. This hypothesis was confirmed by the internal friction measurements. The amplitude dependence of the logarithmic decrement is shown in figure 6.

High values of decrement estimated for $Mg+ZrO_2$ are due to sliding at the interface between ZrO_2 np and matrix. The interface sliding is the effective damping source. The weak bonding between the magnesium matrix and zirconia nanoparticles is the reason for high values of decrement. On the other hand, low values of decrement estimated for $Mg+Al_2O_3$ indicate a good bonding at the interface, which was also manifested by a higher deformation stresses. Mg reacts strongly with oxide producing MgO or spinels such as $MgAl_2O_4$. On the other hand, bonding between Mg and zirconia particles is weaker. Sliding in the interface between Mg and ZrO_2 is a reason for a high decrement value and consequently also for worse mechanical properties compared with $Mg\text{-}Al_2O_3$ nanocomposite.

Reinforcing particles reported in this study can be divided into two groups. While $\delta\text{-}Al_2O_3$ exhibits tetragonal and ZrO_2 the monoclinic structure; Gr and hBN exhibit the hexagonal structure where well bonded basal planes are stacked in the hexagonal cell, with a weak bonding in the <c> axis direction. On the other hand, the effect of Gr and hBN nanoparticles is different. Reischer et al [19] have reported that the graphite-like nanostructure and chemical inertness of the BN may serve as interlayer material in metal matrix composites with focus on the possibilities of an interlayer texturing. We consider that the BN (and/or Gr) coating of Mg grains created during milling may screens the stress transfer inside grains. Hard hBN interlayers influence the deformation behaviour and contribute to the high strengthening of the Mg+BN nc. In materials with the ultrafine grains (lower than 1μm), grain boundary sliding may contribute to the total strain, especially at elevated temperatures. This process is in the Mg+BN and Mg+Gr nc very probably restricted due to strengthening of grain boundaries with the nanoparticles and their agglomerates. Hard hBN layers well bonded to the Mg grains hinder sliding of the grain boundary dislocations and grain boundary diffusion.

All materials contained 3 vol.% of nanoparticles and were prepared with the same technology. Results show that properties of individual nanocomposites are different. Models calculating stresses necessary for deformation of composites which take into account yield stress in the matrix, particles size and geometry, thermal expansion coefficient of the reinforcing phase are not able to explain difference between composites with various nanoparticles. There are other factors which should be taken into account constructing models characterise the strengthening of nanocomposites.

4. Conclusions

Mechanical and physical properties of various magnesium based nanocomposites were studied. Composites containing 3 vol% of the reinforcing phase nanoparticles were prepared with the same technology. Significant differences between various composites were found. Large – scale application of nanocomposites requires better understanding of processes influencing resulting mechanical and physical properties of nanocomposites. Binding between particles and matrix plays an important role for the resulting properties. Graphite and graphite like structure of hBN serve as interlayer material which screens the stress transfer between the individual grains and contribute to the high deformation stresses. Models calculating the stress necessary for deformation of composites may take into account these circumstances.

Acknowledgments

Authors gratefully acknowledge the financial support from the Charles University under grant PROGRES Q47.

References

[1] Dieringa H 2011 Properties of magnesium alloys reinforced with nanoparticles and carbon nanotubes: A review *J. Mater. Sci.* **46** 289-306

[2] Chen Y, Tekumalla S, Guo Y B, Shabadi R, Shim V P W and Gupta M 2017 The dynamic compressive response of a high-strength magnesium alloy and its nanocomposite *Mater. Sci. Eng. A* **702** 65-72
[3] Ferkel H and Mordike B L 2001 Magnesium strenghthened by SiC nanoparticles *Mater. Sci. Eng. A* **298** 193-9
[4] Trojanová Z, Lukáč P, Ferkel H, Mordike B L and Riehemann W 1997 Stability of microstructure in magnesium reinforced by nanoscaled alumina particles *Mater. Sci. Eng.* **234** 798-801
[5] Haasen S F and Gupta M 2008 Effect of submicron-sized Al_2O_3 particulates on microstructural and tensile properties of Mg *J. Alloy Compd.* **457** 244-50
[6] Gupta M and Wong W L E 2015 Magnesium-based nanocomposites: Lightweight materials of the future *Mater. Charact.* **105** 30-46
[7] Thostenson E T, Li C and Chou T W 2005 Nanocomposites in contex *Compos. Sci. Technol.* **65** 491-516
[8] Jayakumar J, Raghunath B K and Rao T H 2012 Recent development and challenges in synthesis of magnesium matrix nano composites - A review *Int. J. Latest Res. Sci. Technol.* **1** 164-71
[9] Zhao C, Wu H, Ni J, Zhang S and Zhang X 2017 Development of PLA/Mg composite for orthopedic implant: Tunable degradation and enhanced mineralization *Compos. Sci. Technol.* **147** 8-15
[10] Gupta M and Wong W L E 2014 An insight into processing and characteristic of magnesium based composites *Magnes. Technol.* (John Willey & Sons, Inc.) p 419-28
[11] Tjong S C 2007 Novel nanoparticle-reinforced metal matrix composites with enhanced mechanical properties *Adv. Eng. Mater.* **9** 639-52
[12] Cole G D 2003 Magnesium *Chem. Eng. News archive* **36** 52
[13] Casati R and Vedani M 2014 Metal matrix composites reinforced by nano particles – A review *Metal (Basel)* **4** 65-83
[14] Hassan S F, Tan M J and Gupta M 2008 High temperature tensile properties of Mg/Al_2O_3 nanocomposite *Mater. Sci. Eng. A* **486** 56-62
[15] Trojanová Z, Lukáč P, Száraz Z and Drozd Z 2014 Mechanical and accoustic properties of magnesium based alloys (nano)composites prepared by powder metallurgical routes Waldemar A Monteiro ed. *Light Metal Alloys Applications InTech* pp 163-97
[16] Köster W and Rosenthal K 1940 Der Verlauf des elastizitätsmoduls in den systemen des magnesiums mit zink, aluminium, zinn, blei, antimon und wismut *Z. Metallkd.* **32** 163-4
[17] http://konsys-t.tanger.cz/files/proceedings/metal_00/papers/135.pdf
[18] https://www.ceramicindustry.com/ext/resources/pdfs/2013-CCD-Material-Charts.pdf
[19] Reischer F, Pippel E, Woltersdorf J, Stockel S and Marx G 2007 Carbon fibre-reinforced magnesium, Improvement of bending strength by nanodesign of boron nitride interlayers *Mater. Chem. Phys.* **104** 83-7